RELATION BETWEEN ELASTICITY AND MOLECULAR STRUCTURE OF NEMATIC LIQUID CRYSTALS

F. Leenhouts, H. Roebers, A. Dekker, J. Jonker

RELATION BETWEEN ELASTICITY
AND MOLECULAR STRUCTURE OF NEMATIC LIQUID CRYSTALS

F. LEENHOUTS, H. J. ROEBERS, A. J. DEKKER and J. J. JONKER

Solid State Physics Laboratory, Materials Science Center, University of Groningen, The Netherlands

Résumé. — Nous avons mesuré les constantes de Frank d'un nombre de bases de Schiff. Nous observons que le paramètre K_{33}/K_{11} diminue si la longueur de la chaîne alkyle s'accroît. Les résultats indiquent que les constantes sont reliées aux dimensions moléculaires et peuvent être expliquées à l'aide de la théorie de Priest.

Abstract. — Experimental values are reported for the elastic constants of a number of Schiff's bases. The ratio K_{33}/K_{11} is found to decrease with increasing alkyl chain length. The results indicate that the elastic constants are related to the molecular dimensions and can be understood qualitatively in terms of the theory of Priest.

1. **Introduction.** — According to the theory developed by Zocher, Oseen and Frank [1], the elastic distortion free energy density is given by :

$$F_d = \frac{1}{2} \left[K_{11}(\nabla \cdot \mathbf{n})^2 + K_{22}(\mathbf{n} \cdot \nabla \times \mathbf{n})^2 + K_{33}(\mathbf{n} \times \nabla \times \mathbf{n})^2 \right] \tag{1}$$

where the elastic constant K_{11} refers to splay, K_{22} to twist and K_{33} to bend. Like many other physical properties of liquid crystals, the elastic constants may be expected to be related to the molecular structure. Systematic experimental studies of this relationship are still scarce. However we should mention the measurements of de Jeu *et al.* [2] on two homologous series, *viz.* the p,p'-di-n-alkyl and p,p'-di-n-alkoxy azoxybenzenes and of Karat *et al.* [3] on a number of cyanobiphenyls.

In this paper we report measurements of the elastic constants of a number of Schiff's bases of the type

CH₃O—⟨◯⟩—CH=N—⟨◯⟩—R₂
         R₁
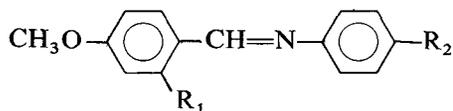
A list of abbreviations and nematic ranges of these compounds is given in table I. The compounds belonging to the same homologous series as APAPA have been abbreviated as APAPAn where n is the number of carbons of the alkyl chain attached to the OCO-group.

Assuming cylindrical symmetry of the molecules, the orientational distribution function only depends on the angle θ between the long molecular axis and $\mathbf{n}$. The degree of order can be specified by the parameters $\langle P_{2n}(\cos \theta) \rangle$ where P_{2n} represents the

TABLE I

List of liquid crystals studied. T_m and T_c are the transition temperatures crystal-nematic and nematic-isotropic. R_1 and R_2 represent the side- and endgroups respectively

Abbreviation	R_1	R_2	T_m (°C)	T_c (°C)
OHMBBA	OH	C_4H_9	44	64.6
MBBA	H	C_4H_9	18	46.2
MBCA	H	CN	106	118.0
APAPA	H	$OCOCH_3$	82	111.0
APAPA2	H	$OCOCH_2CH_3$	72	110.6
APAPA3	H	$OCO(CH_2)_2CH_3$	53	112.8
APAPA4	H	$OCO(CH_2)_3CH_3$	61	100.0
APAPA5	H	$OCO(CH_2)_4CH_3$	83	103.2

Legendre polynomial of degree $2n$ and the brackets denote a statistical average. The first calculations of elastic constants carried out by Saupe and Nehring [4, 5] were based on the mean field theory of Maier and Saupe [6] ; they calculated that

$$K_{ii} = C_{ii} \langle P_2 \rangle^2 / V^{7/3} \tag{2}$$

where the C_{ii} are constants depending on molecular properties and V is the molar volume. They predict :

$$K_{11} : K_{22} : K_{33} = 5 : 11 : 5 . \tag{3}$$

The expressions (2) and (3) were obtained for the special case of the London-Van der Waals dispersion forces. Priest [7] extended this work to an arbitrary intermolecular interaction. Retaining the assumption of axial symmetry but including higher order terms he derived :

$$K_{11} = \overline{K}[1 + \Delta - 3\,\Delta'(\langle P_4 \rangle/\langle P_2 \rangle) + \cdots]$$

$$K_{22} = \overline{K}[1 - 2\,\Delta - \Delta'(\langle P_4 \rangle/\langle P_2 \rangle) + \cdots] \qquad (4)$$

$$K_{33} = \overline{K}[1 + \Delta + 4\,\Delta'(\langle P_4 \rangle/\langle P_2 \rangle) + \cdots]\,.$$

Here $\overline{K} = (K_{11} + K_{22} + K_{33})/3$ is proportional to $\langle P_2 \rangle^2$. The quantities Δ and Δ' are related to molecular properties ; for the case of hard spherocylinders (cylinders capped with hemispheres at both ends) interacting via a hard core repulsion, Priest found :

$$\Delta = (2\,R^2 - 2)/(7\,R^2 + 20)$$
$$\Delta' = 27(R^2/16 - 1/6)/(7\,R^2 + 20) \qquad (5)$$

In these expressions $R = l/b$, where $(l + b)$ and b are the overall length and breadth of the spherocylinders.

2. Experimental. — 2.1 FREEDERICKSZ TRANSITION.

— We have measured the elastic constants by observing the distortion of a uniformly aligned nematic slab in a magnetic field. If the director of the undistorted nematic layer is oriented perpendicular to the magnetic field the nematic will undergo a distortion as soon as the field exceeds a critical value H_c. Assuming strong anchoring of the molecules at the sample boundaries the critical field is given by [8]

$$(H_c)_{ii} = (\pi/d)\,(K_{ii}/\Delta\chi)^{1/2}\,, \quad i = 1, 2, 3\,, \qquad (6)$$

where d is the thickness of the layer, $\Delta\chi = \chi_\parallel - \chi_\perp$ the difference between the volume susceptibilities parallel and perpendicular to the director. The experimental geometries represented in figure 1a, 1b and 1c correspond to splay, twist and bend respectively.
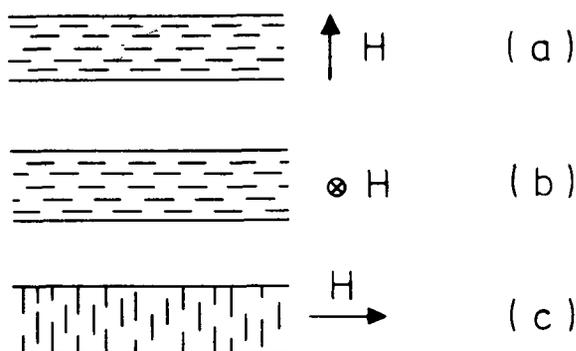

FIG. 1. — Experimental configurations for determining the critical field for splay (a), twist (b) and bend (c).

2.2 TWIST.

— We have measured the twist elastic constant using the conoscopic method [9]. The details of this method and the experimental set up have been described in a previous paper [10]. A planar oriented nematic single crystal, placed between a polarizer and an analyzer and illuminated by a cone of convergent monochromatic light exhibits an inter-ference pattern consisting of hyperbolas. If a twist is induced by means of a magnetic field, applied perpendicular to the director of the undistorted nematic, the pattern rotates by an amount δ given by [9]

$$\delta = \frac{1}{2}\ \text{arctan} \times$$
$$\times\ [2\sin\theta_m/(2\ E(\pi/2, \sin\theta_m) - F(\pi/2, \sin\theta_m))] \qquad (7)$$

with

$$F(\pi/2, \sin\theta_m) = (\pi H/2\ H_c) \qquad (8)$$

F and E are complete elliptic integrals of the first and second kind and θ_m the twist angle in the middle of the sample. In figure 2 we have shown the rotation-angle δ as a function of the magnetic field. The crosses represent measurements and the solid curve is a least squares fit using eqs. (7) and (8) with H_c as parameter.
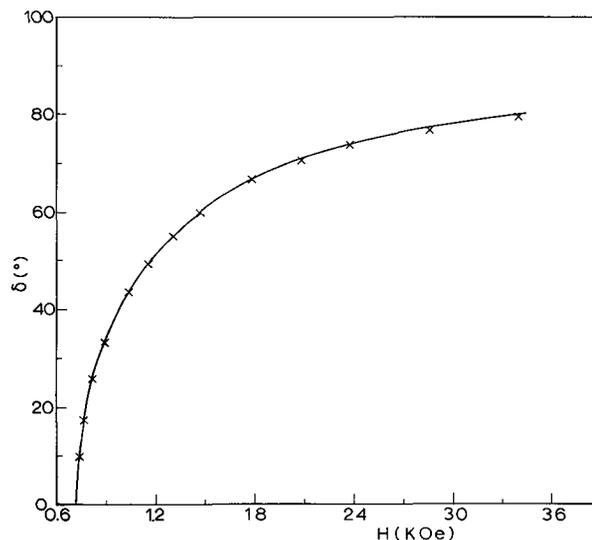

FIG. 2. — The rotation angle δ of the interference pattern as a function of the magnetic field. The crosses represent measurements and the solid curve is a least squares fit according to eqs. (7) and (8).

2.3 BEND AND SPLAY.

— The bend and splay elastic constants were measured by employing the method developed by Saupe [8]. One measures the intensity of a monochromatic laser beam (HeNe, 6 328 Å) which traverses a uniformly oriented liquid crystal placed between crossed polarizers. If the director of the undistorted sample is perpendicular to the field, the intensity shows maxima and minima as soon as the field exceeds a critical value H_c. In fact, one measures the phase difference δ between two components of plane polarized light propagating normal to the nematic layer. Consider for instance configuration 1a. The interrelation between the distortion, the magnetic field and the phase difference δ is given by [8]

$$\delta = n_e\, d\left[1 - (2\,H_c/\pi H)\right.$$

$$\times \int_0^{\pi/2}\left[\frac{(1 + \gamma\sin^2\theta_m\sin^2\psi)}{(1 - \sin^2\theta_m\sin^2\psi)(1 + \nu\sin^2\theta_m\sin^2\psi)}\right]^{1/2}\left.\mathrm{d}\psi\right]$$

$$(9)$$

with

$$H/H_c = (2/\pi)\,\Pi(\alpha^2, k)/(1 + \gamma\sin^2\theta_m)^{1/2}\,. \quad (10)$$

Here $\sin\psi = \sin\theta/\sin\theta_m$ where θ is the angle between the director and the zero field alignment direction; θ_m is the value of θ in the middle of the sample;

$$\gamma = (K_{33} - K_{11})/K_{11}\,;$$
$$\alpha^2 = \gamma\sin^2\theta_m/(1 + \gamma\sin^2\theta_m)\,;$$
$$k^2 = (1 + \gamma)\sin^2\theta_m/(1 + \gamma\sin^2\theta_m)$$

and

$$\nu = (n_e^2 - n_o^2)/n_o^2$$

where n_o and n_e are the ordinary and extraordinary refractive indices respectively. $\Pi(\alpha^2, k)$ is the complete elliptic integral of the third kind. The values of δ corresponding with the extrema of the transmitted light can be calculated readily. Using the known values of n_e and n_o we fitted eqs. (9) and (10) to the data with H_c and the ratio K_{33}/K_{11} as parameters. We used a least squares fitting program, developed by Deuling [11]. Hence it is possible to obtain in this way both K_{11} (from H_c) and the ratio K_{33}/K_{11}. Eqs. (9) and (10) apply also to configuration 1c (bend) if n_e and n_o as well as K_{11} and K_{33} are interchanged.

The following points were found to be important for an accurate determination of H_c :

a) Strong anchoring of the molecules at the sample boundaries. The formulas (7)-(10) were derived under the assumption of strong anchoring (see section 2.4).

b) The variation of the magnetic field should be quasi-static. We limited the scanning rate of the field to about 13 Oe/min.

c) The magnetic field direction must be exactly perpendicular to the zero field alignment direction. If H is not perpendicular to $\mathbf{n}(H = 0)$ the δ vs. H curve shows a tail near H_c. Applying formulas (7)-(10) in that case results in a value of H_c which is too low.

2.4 BOUNDARY CONDITIONS. — In order to obtain nematic single crystals the glass surfaces must be treated in a special way. Spruijt [12] and de Jeu et al. [13] have shown that the thresholdfield depends on the surface treatment given, because the anchoring energy differs for the various treatments. Homeotropic single crystals were obtained by heating the glass plates in 1-dodecanol at 200 °C for about 30 min. Planar samples were obtained in two different ways. First we used the well known rubbing technique to create an easy direction, while in addition the sur-

factant $CH_3(CH_2)_{15}(OCH_2CH_2)_{20}OH$ (cremaphor O, BASF), was added. However the cremaphor did not stick to the surface at high temperatures, thus spoiling the alignment. For measurements above 80 °C we therefore used glass plates coated with a polymer film of poly-p-xylylene (—CH_2—Ph—CH_2—)$_n$ which were gently rubbed afterwards. For the compounds studied both techniques used to obtain planar samples were found to give the same thresholds. In comparing different treatments Spruijt [12] and de Jeu et al. [13] observed that the heighest thresholds were observed for the techniques described above. However the question still remains whether it is justified to assume strong anchoring. A convincing argument for this can be derived from figure 2. The form of the curve merely depends on the geometry chosen and the only parameter is H_c. Since the curve fits the points quite well even up to high fields, we must conclude that strong anchoring indeed exists. In section 2.3 we have shown that both $K_{11}/\Delta\chi$ and $K_{33}/\Delta\chi$ can be evaluated from a least squares procedure using eqs. (9) and (10). In addition $K_{33}/\Delta\chi$ can be determined directly for the homeotropic samples. We have found that the values of $K_{33}/\Delta\chi$ measured directly were not lower than those obtained from the computer-fit. Hence we are confident that the condition of strong anchoring is fulfilled for the homeotropic case also.

2.5 ADDITIONAL MEASUREMENTS. — Eq. (6) shows that not only H_c but also d and $\Delta\chi$ must be known in order to calculate K_{ii}. The thickness d was determined interferometrically [10]. The anisotropy of the mass susceptibility $\Delta\chi^g = \Delta\chi/\rho$, where ρ is the density, was measured at the Philips Research Laboratories, using the Faraday method. The densities were measured in this laboratory. The data of $\Delta\chi$ and ρ will be published in the near future. The ordinary refractive index n_o was measured by means of an Abbe refractometer. The birefringence $\Delta n = n_e - n_o$ was determined using a combination of two optical techniques [14].

3. Results. — The compounds studied were purified before use by means of recrystallization from methanol. The parameters $K_{33}/\Delta\chi$ were derived from the threshold fields H_c (Fig. 1c) with the exception of MBCA and APAPA5, because we could not obtain proper homeotropic samples for these compounds. In these cases K_{33} was calculated using eqs. (9) and (10). The estimated accuracy of the elastic constants is about 4 % for those derived from H_c. The values of K_{33} obtained indirectly from the computerfit showed a somewhat greater scatter ; the accuracy is about 7 %.

In figure 3 we have plotted the reduced elastic constants C_{ii} of MBBA, defined in eq. (2) ; they were calculated using values of $\langle P_2 \rangle$ derived from measurements of the mass susceptibility. Assuming
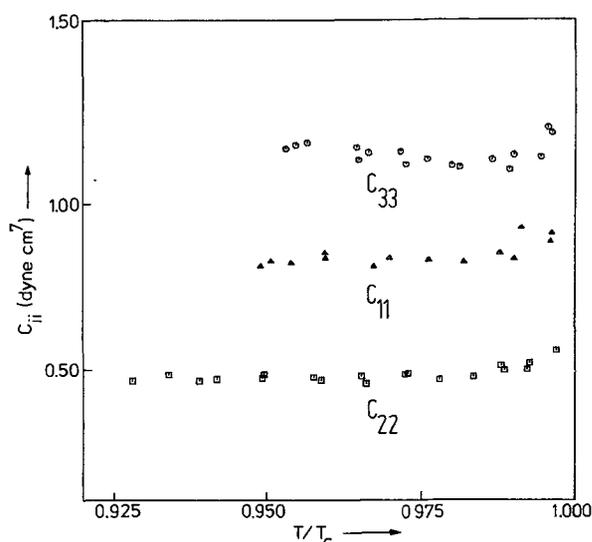
FIG. 3. — The reduced elastic constants as a function of the reduced temperature for MBBA.

axial symmetry of the molecules the anisotropy of the mass susceptibility $\Delta\chi^g$ can be written as [15]

$$\Delta\chi^g = N_A \, \Delta\chi_m \langle P_2 \rangle / M \,. \qquad (11)$$

Here N_A is Avogadro's number, M the mass number and $\Delta\chi_m$ the anisotropy of the susceptibility of an isolated molecule. We have used the value

$$61.2 \times 10^{-6} \ \mathrm{cm^3/mol}$$

for $N_A \, \Delta\chi_m$ [16], obtained from measurements on a solid single crystal of PAA. Figure 3 shows that C_{11} and C_{22} increase slightly with temperature, while C_{33} decreases somewhat. However the temperature dependence is weak and we conclude that the elastic constants are roughly proportional to $\langle P_2 \rangle^2$, in agreement with eq. (2). The elastic constants of the other compounds studied exhibit a similar temperature dependence.

Now we will compare the elastic constants of the various compounds. In table II we have collected the data at the same reduced temperature, i.e. at $T/T_c = 0.960$. We start with a comparison of MBBA, APAPA and MBCA which only differ in

TABLE II

Elastic constants of the compounds studied at
$$T/T_c = 0.960$$

	K_{11}	K_{22}	K_{33}	$\overline{K}$	K_{33}/K_{11}	K_{22}/K_{11}
	(10^{-7} dyne)					
OHMBBA	6.31	3.84	6.67	5.61	1.06	0.61
MBBA	5.06	3.19	6.85	5.03	1.35	0.63
MBCA	7.27	4.66	13.89	8.61	1.91	0.64
APAPA	6.25	4.47	13.20	7.97	2.11	0.72
APAPA2	5.73	4.21	10.28	6.74	1.79	0.73
APAPA3	6.71—	.4.39	11.30	7.47	1.68	0.65
APAPA4	6.59	4.12	8.45	6.39	1.28	0.63
APAPA5	7.60	4.52	10.55	7.56	1.39	0.59

the endgroup attached to the aniline ring at the paraposition.

Evidently a change in the endgroup strongly affects the bending constant (Fig. 4), but hardly affects the splay and twist constants. We note in particular the large bending constant associated with the rigid CN and $OCOCH_3$ groups. Also note that incorporation of OH as a sidegroup in MBBA has no influence on K_{33}, but affects noticeably the splay and twist parameter.
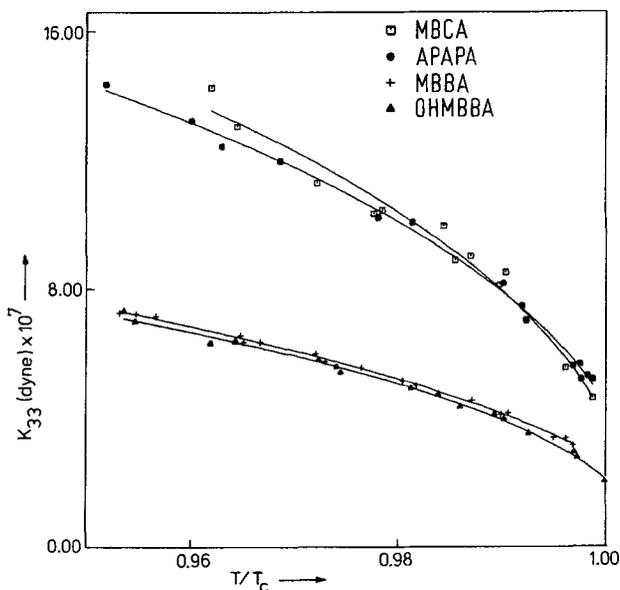

FIG. 4. — The bend elastic constant K_{33} as a function of the reduced temperature for MBCA, APAPA, MBBA and OHMBBA.

Comparing the homologues of APAPA we note that K_{33} decreases somewhat if the number of carbons of the chain increases whereas K_{11} and K_{22} increase. In addition we observe the well known even-odd alternation, which is related to the position of the carbon chain with respect to the long molecular axis.

Inspection of tables I and II shows that the height of $\overline{K} = (K_{11} + K_{22} + K_{33})/3$ is clearly related to the clearing temperature. This is not surprising. As pointed out by de Gennes [17] one expects on the basis of a purely dimensional argument that the elastic constants should be proportional to U/a, where U is a typical molecular interaction energy and a is a molecular dimension. The clearing temperature will be related to U whereas a is expected to be about the same for all materials studied.

4. **Discussion.** — The molecules of the nematic materials studied in this paper have a common rigid core and differ only in their end groups, which show considerable variations in dipole moment, chain length and flexibility. Since at this stage the interpretation of the elastic properties in terms of specific features of the molecular structure is out of question,

it seems appropriate to attempt first to relate trends in these properties qualitatively to the overall shape. For this purpose the theory of Priest [7] seems to provide a suitable basis ; the specific model involved in the Saupe-Nehring calculations may be disregarded because our results by no means satisfy the predicted ratio's expressed by eq. (3).

4.1 THE RATIO K_{33}/K_{11}. — In figure 5 we have plotted K_{33}/K_{11} as a function of R using eqs. (4) and (5). If $\langle P_4 \rangle / \langle P_2 \rangle > 0$ we observe that K_{33}/K_{11}
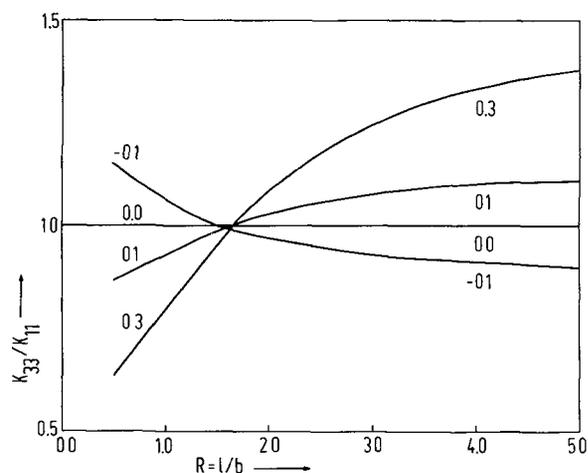

FIG. 5. — Ratio of the bend and splay elastic constant K_{33}/K_{11} as a function of the length to breadth ratio R for spherocylinders according to eqs. (4) and (5). The numbers accompanying the curves represent values of $\langle P_4 \rangle / \langle P_2 \rangle$.

decreases with decreasing length to width ratio. At first sight figure 5 is not in agreement with the results of table II where we observe a decrease of K_{33}/K_{11} for an increasing number of carbons of the alkyl chain. However it is well known that the chain is flexible to some extent and can adopt a great number of possible conformations, characterized by rotations around the carbon-carbon bonds. The rotation potential of a particular bond has three minima, defining for each bond the three possible states, i.e. the planar trans state (t) and the two symmetrical gauche states (g$^+$, g$^-$) obtained by a rotation around the bond of about $\pm$ 120°. Assuming nearest neighbour interaction between the chain segments the internal energy may be written as [18] :

$$E_{int} = \sum_{i=1}^{n-1} E(\xi_{i-1}, \xi_i) \qquad n = 2, 3, ... \qquad (12)$$

Here ξ = t, g$^+$ or g$^-$ and n is the number of carbons of the chain. Figure 6 shows the molecular structure of APAPAn in its planar trans configuration. The bond connecting the OCO-group and the first carbon of the chain (ξ_0) is assumed to be in the trans state. The angle β is 6.5° [19] in APAPA. The axis A is parallel to the line joining the odd or even numbered carbons of the chain in its trans configuration. In order
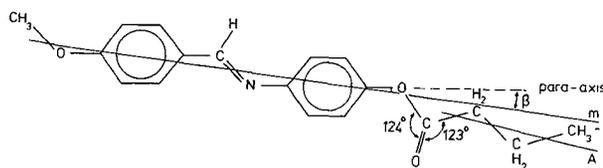

FIG. 6. — The molecular structure of the homologues of APAPA.

to describe the dimensions of the chain we associate with it a length l_c corresponding to the maximum projection of the chain on the A-axis and a breadth b_c corresponding to the average of the maximum projection on the trans plane and the maximum projection on an axis normal to this plane. Using eq. (12) and the values $E(\xi, t) = 0$,

$$E(t, g^{\pm}) = E(g^{\pm}, g^{\pm}) = 400 \text{ cal/mol}$$

and $E(g^{\pm}, g^{\mp}) = 2\,200$ cal/mol corresponding to polymethylene [18] we have calculated $R_c = \langle l_c/b_c \rangle$ and $\langle l_c \rangle/n$ where the brackets denote a statistical average over all possible conformations. The hydrogen atoms of the chain are included in this calculation. Table III collects the results. Note that $\langle l_c/b_c \rangle$ first increases somewhat and decreases for longer chains. However, a rigid chain will be characterized by a strong increase of the length to width ratio. We note that the length to width ratio of the chain does not show the well known odd-even effect. This effect would have been observed if the chain had been projected on the long molecular axis m. However the angle between A and m is small. Therefore the length of the projection on A will not differ much from the length of projection on m. The calculation of R_c applies to an isolated molecule. Interaction between neighbouring molecules, which will have an ordering effect on the chain [20], has been neglected. However it follows from NMR measurements [21] that the order parameter of the chain segments decreases as the segments are further away from the core as a result of the flexibility. So the results given in table III reflect at least qualitatively this feature of the chain. Consequently we may

TABLE III

The parameters $\langle l_c/b_c \rangle$ and $\langle l_c \rangle/n$ of an alkyl chain consisting of n carbons

n	$\langle l_c/b_c \rangle$	$\langle l_c \rangle/n$ (Å)
1	1.08	2.15
2	1.16	1.36
3	1.27	1.15
4	1.28	1.01
5	1.27	0.92
6	1.25	0.84
7	1.22	0.79
8	1.19	0.74

consider the molecules as composed of a rigid lathlike core and an alkyl chain which tends towards a spherical shape as its length increases. However it is difficult to associate a length and width to the molecule as a whole, because of the irregular shape of its structure. Nevertheless the results of table III suggest that increasing the number of carbons of the chain results in a reduction of the effective length to width ratio R. Figure 5 predicts in this case a decrease of K_{33}/K_{11}, which is in agreement with the data. Comparing the other compounds of table II we note that K_{33}/K_{11} is about equal for MBBA and APAPA4 both having an alkyl chain consisting of 4 carbons. Comparing OHMBBA and MBBA we can expect that K_{33}/K_{11} of OHMBBA is lower than K_{33}/K_{11} of MBBA as a result of the presence of an ortho OH-group which adds to the width of the molecule. From a molecular model we can understand that the length to width ratio of the MBCA-molecule is somewhat lower than this ratio of the APAPA-molecule. The ratio K_{33}/K_{11} of MBCA is indeed somewhat lower.

Next we consider the temperature dependence of K_{33}/K_{11}. Figure 5 predicts that K_{33}/K_{11} decreases with increasing temperature, i.e. decreasing ratio $\langle P_4 \rangle / \langle P_2 \rangle$, if $K_{33} > K_{11}$ but increases if $K_{33} < K_{11}$. The temperature dependence is weak if $K_{33} \simeq K_{11}$. In figure 7 we have given the ratio K_{33}/K_{11}
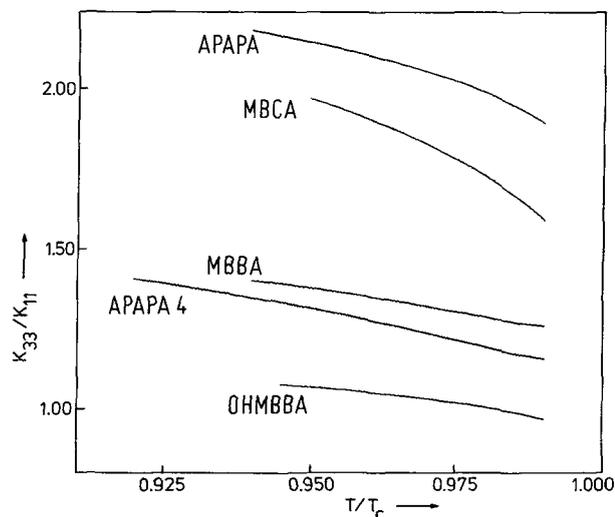

FIG. 7. — The ratio of the bend and splay elastic constant as a function of the reduced temperature for APAPA, MBCA, MBBA, APAPA4 and OHMBBA.

of a number of materials. The dependence on temperature agrees with figure 5.

De Jeu et al. [2] have measured the elastic constants of two homologous series of azoxy compounds. In agreement with our measurements they have found that K_{33}/K_{11} decreases with increasing chain length. In agreement with figure 5 they found that K_{33}/K_{11} increases with increasing temperature if $K_{33} < K_{11}$.

4.2 THE RATIO K_{22}/K_{11}. — Table II shows that the differences between the parameters K_{22}/K_{11} of the various compounds are small. We have found $K_{22} < K_{11}$ in agreement with eq. (4). The temperature dependence of K_{22}/K_{11} is small. Eq. (4) has been derived under the assumption of axial symmetry of the molecules. However the molecules are more or less lathlike in shape depending on the bridging group connecting the two benzene rings. For instance it is well known that the two benzene rings of the MBBA molecule are not coplanar [22]. The angle between the rings is about 45°. One might expect that the ratio K_{22}/K_{11} depends on the character of the bridging group, i.e. reflects the deviation from axial symmetry around the long molecular axis. In this respect it is of interest to mention that we have measured K_{22} of p-p'-diheptylazobenzene [23] using the conoscopic method. In this material the two benzene rings are coplanar. We found that the ratio K_{22}/K_{11} of this material is about 0.40, which is substantially lower than K_{22}/K_{11} of the compounds listed in table II. Accurate measurements of K_{22} are still scarce. Therefore more experimental data are necessary to prove a possible relation between K_{22}/K_{11} and the deviation from axial symmetry.

References

[1] OSEEN, C. W., Trans. Faraday Soc. 29 (1933) 883.
    ZOCHER, H., Trans. Faraday Soc. 29 (1933) 945.
    FRANK, F. C., Disc. Faraday Soc. 25 (1958) 19.
[2] DE JEU, W. H., CLAASSEN, W. A. P., J. Chem. Phys. 67 (1977) 3705.
[3] KARAT, P. P., MADHUSUDANA, N. V., Mol. Cryst. 36 (1976) 51.
[4] SAUPE, A., Z. Naturforsch. 15a (1960) 810.
[5] NEHRING, J., SAUPE, A., J. Chem. Phys. 56 (1972) 5527.

[6] MAIER, W., SAUPE, A., Z. Naturforsch. 13a (1958) 564 ; 14a (1959) 882 ; 15a (1960) 287.
[7] PRIEST, R. G., Phys. Rev. A 7 (1973) 720.
[8] SAUPE, A., Z. Naturforsch. 15a (1960) 815.
[9] CLADIS, P. E., Phys. Rev. Lett. 28 (1972) 1629.
[10] LEENHOUTS, F., VAN DER WOUDE, F., DEKKER, A. J., Phys. Lett. 58A (1976) 242.
[11] DEULING, H., private communications.

[12] SPRUIJT, A. M. J., Freiburger Arbeitstagung Flüssigkristalle (1976) 14.

[13] DE JEU, W. H., CLAASSEN, W. A. P., SPRUIJT, A. M. J., *Mol. Cryst. Liq. Cryst.* **37** (1976) 269.

[14] LEENHOUTS, F., VAN DER WOUDE, F., accepted for publication in *J. Physique Lett.*

[15] STEPHEN, M. J., STRALEY, J. P., *Rev. Mod. Phys.* **46** (1974) 677.

[16] FOEX, G., *Trans. Faraday Soc.* **29** (1933) 958.

[17] DE GENNES, P. G., *The Physics of Liquid Crystals* (Clarendon, Oxford) 1974.

[18] FLORY, P. J., *Statistical Mechanics of Chain Molecules* (Interscience, New York) 1969.

[19] VISINTAINER, J. J., BOCK, E., DONG, R. Y., TOMCHUK, E., *Can. J. Phys.* **53** (1975) 1483.

[20] MARČELJA, S., *J. Chem. Phys.* **60** (1974) 3599.

[21] For instance : DELOCHE, B., CHARVOLIN, J., *J. Physique* **37** (1976) 1497.

[22] DONG, R. Y., TOMCHUK, E., WADE, C. G., VISINTAINER, J. J., BOCK, E., *J. Chem. Phys.* **66** (1977) 4121.

[23] DE JEU, W. H., LEENHOUTS, F., *J. Physique* **39** (1978) 15.